MODIS Semi-annual Report (January 2002 – June 2002)

Bo-Cai Gao, Yong Han, Po Li, and Ping Yang

(This reports covers the MODIS **cirrus characterization and correction** algorithm and part of the MODIS **near-IR water vapor algorithm**)

Main topics addressed in this time period:

1. **MODIS near-IR water vapor algorithm**:

The MODIS near-IR water vapor algorithm is now quite stable. During this reporting period, we didn't make any modifications and upgrades to the codes. Instead, we focused on the validation of the Level 2 and Level 3 near-IR water vapor products retrieved from the Terra MODIS data.

In order to gain confidence in the accuracy of our near-IR water vapor products, we have compared the MODIS near-IR water vapor values with those measured with a ground-based upward-looking microwave radiometer located at a site in the Southern Great Plains in Oklahoma for a time period between November 2000 and December 2001. The microwave radiometer measurements were sponsored by the Department of Energy's Atmospheric Radiation Measurement Program and the data were released for public use. Figure 1a shows a scatter plot between the water vapor values measured with the microwave radiometer and the MODIS near-IR water vapor values measured on clear days between November 2000 and December 2001. The data points for column water vapor amounts greater than 3.5 cm are not included in this plot. The regression analysis of the two data sets gives a slope of 0.97 and a very small offset (0.06 cm). Therefore, the agreement between the two sets of data is quite well. Figure 1b shows a similar plot but including all the data points having column water vapor amounts greater than 3.5 cm for the same time period. The regression analysis of the two data sets gives a slope of 0.93. The decrease in the slope is largely due to the fact that for the few points with water vapor values greater than 3.5 cm, the MODIS water vapor values are somewhat systematically larger than the microwave radiometer water vapor values. Overall, the water vapor values from MODIS and from microwave

radiometer measurements, as shown in Figs. 1a and 1b, agree quite well with differences typically in the range between 5 and 10%.

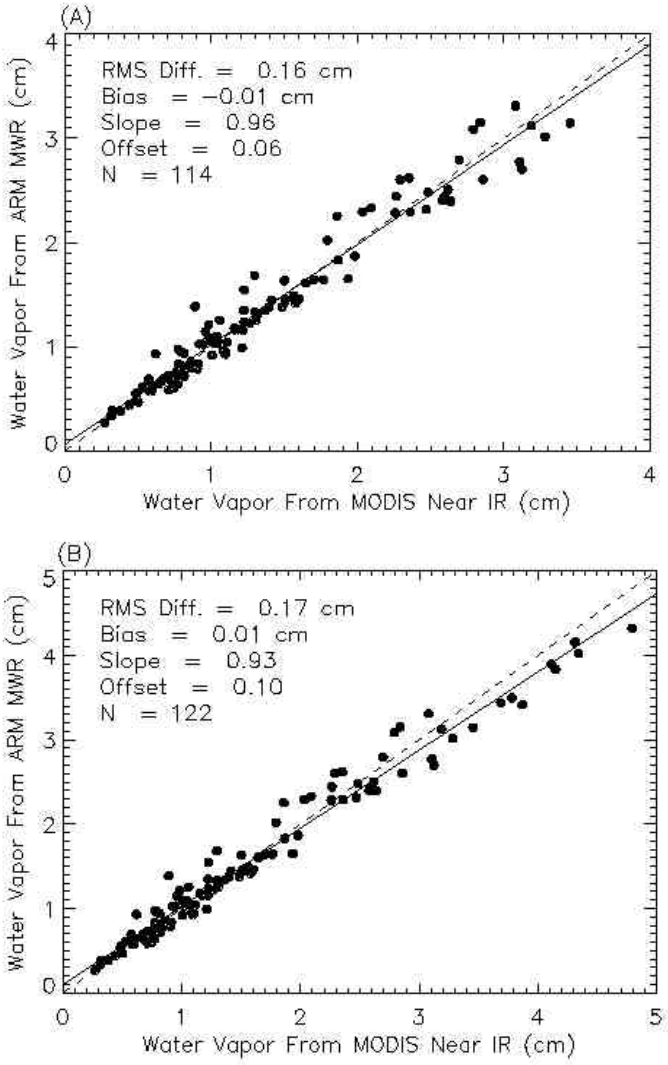

Fig. 1. (a): a scatter plot between the water vapor values measured with a ground-based upward-looking microwave radiometer at a site in the Southern Great Plains in Oklahoma and those retrieved from images of MODIS near-IR channels for a time period between November 2000 and December 2001 and for column water vapor amounts less than 3.5 cm; (b) similar to (a) except that the data points for water vapor amounts greater than 3.5 cm are included in the analysis.

We made additional comparisons and analysis between MODIS near-IR water vapor values and those measured with a microwave radiometer during the

ACE-Asia field experiment by Dr. Si-Chee Tsay's research group of NASA Goddard Space Flight Center. Figure 2 shows an example of such comparisons. On clear days, the two sets of data agreed quite well. The MODIS data can track the water vapor variations very nicely.

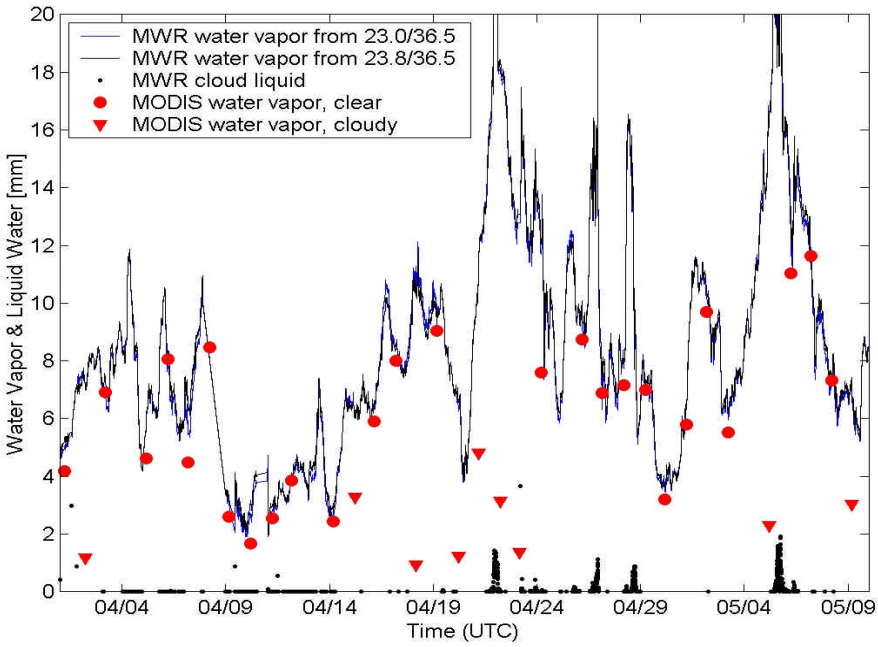

Fig. 2. An example of comparisons between MODIS near-IR water vapor values and those measured with a microwave radiometer during the ACE-Asia field experiment by Dr. Si-Chee Tsay's research group.

We made extensive analysis of the Level 3 near-IR water vapor products. Through analysis of our Level 3 daily, 8-day, and monthly mean water vapor images at a 1° x 1° latitude-longitude equal angle grid, we have found that the monthly-mean Level 3 images allow easy observations of seasonal variations of water vapor distributions. Figures 3a shows a Level 3 water vapor image over the continental U.S., portions of Mexico and Canada for January of 2001. In this winter month, most parts of the U.S. have column water vapor amounts less than 1.5 cm. The State of Florida and the southern part of Texas have column water vapor amounts between approximately 2 and 3 cm. Figure 3b is a Level 3 water vapor image over the same area but for July of 2001. The Rocky Mountain areas have column water vapor values less than about 2 cm in the summer month. Many states in the middle part of the U.S. have high concentrations of water vapor originating from the Gulf of Mexico. The

moisture can even transport through North Dakota and Minnesota to reach Canada. The high concentrations of moisture over the western part of Mexico are due to moisture originated from the Pacific Ocean. The patterns of water vapor distributions for the summer month are drastically different from those for the winter month.

(A)

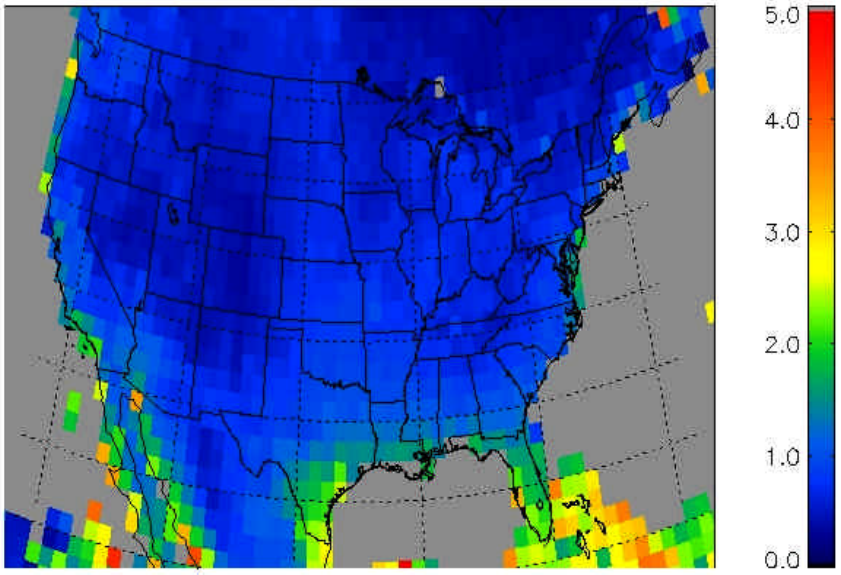

(B)

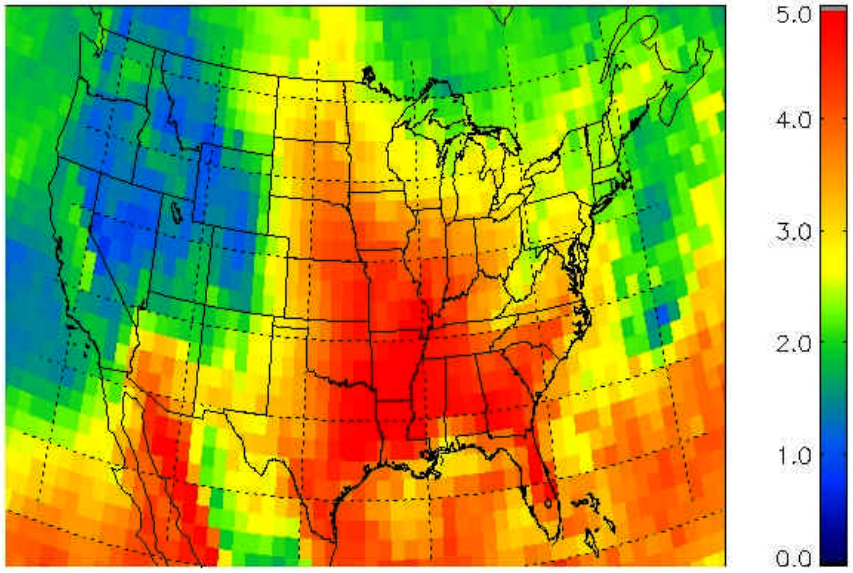

Fig. 3. (a): a monthly-mean Level 3 water vapor image over the continental U.S., portions of Mexico and Canada for January, 2001; (b): similar to (a), except for July, 2001.

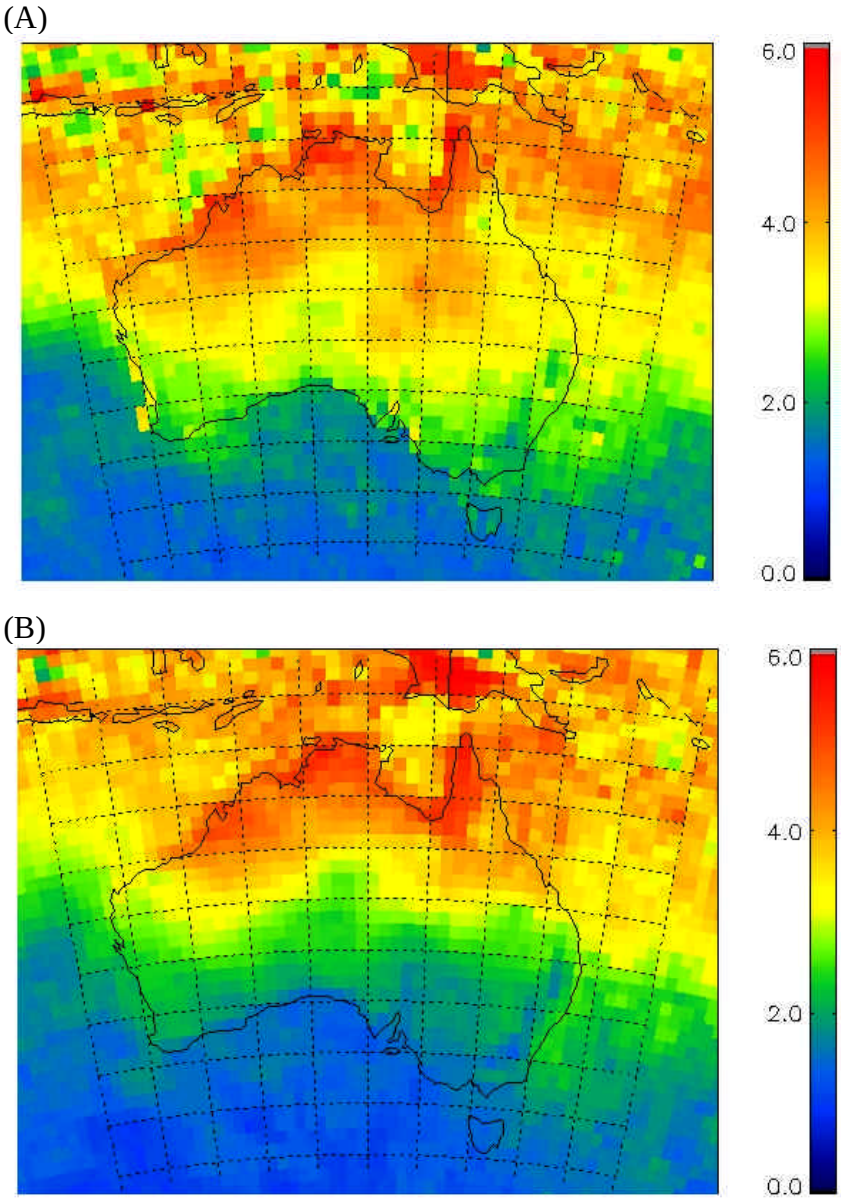

Fig. 4. (a): a monthly-mean Level 3 water vapor image over Australia for January of 2001; (b): similar to (a), except for January of 2002.

The Level 3 monthly-mean near-IR water vapor images can also be used to study annual variations of water vapor distributions. Figure 4 shows an example of such studies. In Fig. 4a we show the Level 3 water vapor image over Australia for January 2001. January is a summer month in the southern hemisphere. The northern part of Australia is in the tropical region. Column water vapor amounts over this region are typically in the 4 – 6 cm range. The southeastern parts of Australia typically have column water vapor amounts between 2 and 3 cm. Fig. 4b shows the water vapor image over Australia for

the same month but for the year of 2002, an El Nino year. By comparing Fig. 4b with Fig. 4a, it is seen that column water vapor amounts in the middle and southern portions of Australia for January of 2002 are significantly less than those for January of 2001. The decreases in water vapor amounts may be related to the eastward movement of the "warm pool" during the El Nino year. The waters north to Australia in the Pacific Ocean are colder in the El Nino year. Less evaporation would occur and less amounts of water vapor would be available for transporting to the Australia continent.

Figure 5a is a global water vapor image for January of 2001. During this northern hemisphere winter month, the water vapor amounts over most parts of North America, Europe, Asia, and northern part of the Africa Continent have small amounts of water vapor (< 2 cm). Only the southern parts of Indian Continent and Indo-China have relatively higher moisture contents with column water vapor amounts in the range of 3 – 4.5 cm. Brazil, southern part of Africa Continent, and Australia have high moisture contents. Figure 5b is a global water vapor image for July of 2001. The northern hemisphere becomes more moist in comparison with the January image. The Indian Continent, Indo-China, and eastern part of China are now saturated with water vapor. The middle part of U.S. is also quite moist due to water vapor transported over from the Gulf of Mexico. The southern part of South America, southern part of the African Continent, and Australia are dry during their winter season. The high elevation areas, such as those of Rocky Mountains in North America, Andes Mountains in South America, Himalayas Mountains in Asia, and the Sahara desert areas in northern Africa have low moisture contents in both the July and January images. The water vapor images in Fig. 5a and 5b clearly demonstrate that the level 3 monthly-mean near-IR water vapor images can be used to study seasonal variations of water vapor globally.

(A)

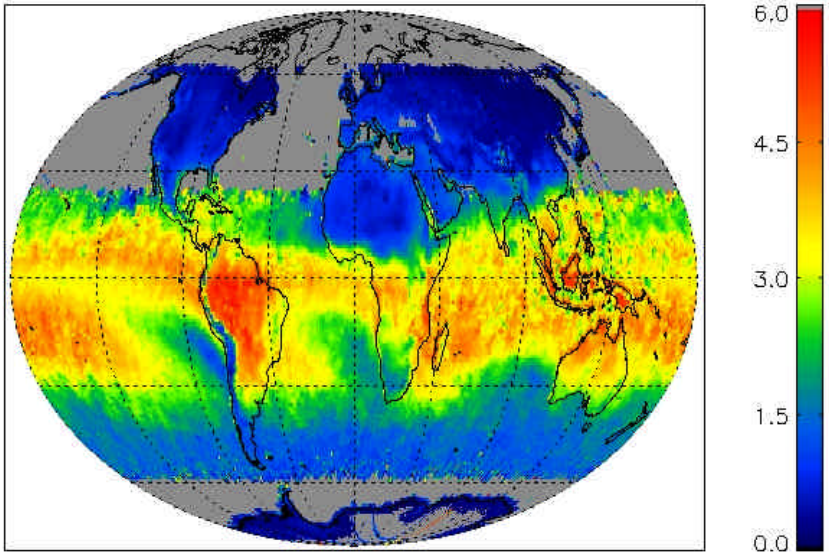

(B)

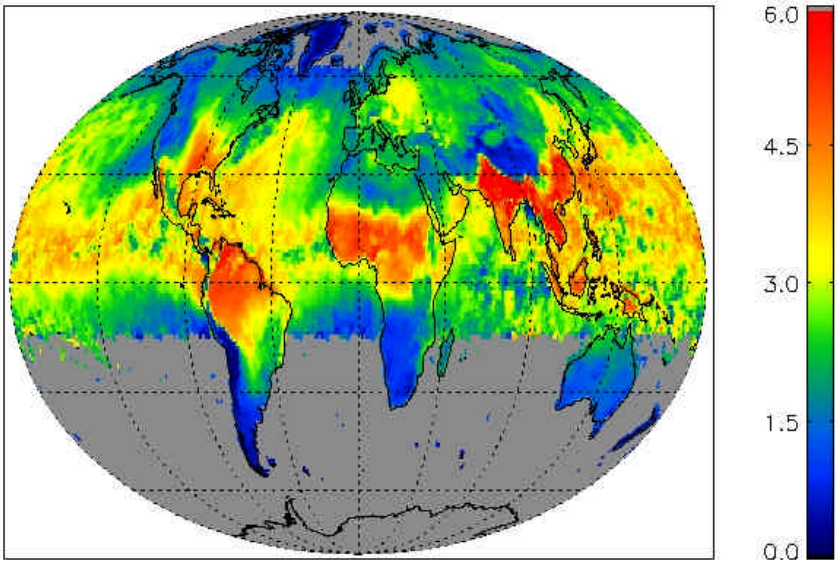

Fig. 5. (a): a monthly-mean global Level 3 water vapor image for January of 2001; (b): similar to (a), except for July of 2001.

2. **MODIS cirrus reflectance algorithms**:

In the present operational version of the cirrus reflectance algorithm, the scatter plot between the 0.645-μm channel and the 1.38-μm channel is used to estimate the transmittance for the water vapor above cirrus that is normally located at an altitude of 8 km or higher. The true cirrus reflectance is obtained from the 1.38-μm band data by scaling the water vapor absorption using the water vapor

transmittance. Since the algorithm is quite stable and results are reasonable, we did not make any modifications and updates to the algorithm during this reporting period. Instead, we concentrated on finishing a paper that describes the algorithm and presents sample results. The paper will appear in the August 2002 issue of IEEE Trans. Geosci. Remote Sensing.

Working closely with Dr. Kaufman's research group at NASA Goddard, an improved cirrus screening method using the 1.24-μm / the 1.38-μm channel ratio for the MODIS aerosol retrieving algorithm has been developed and implemented to the aerosol algorithm.

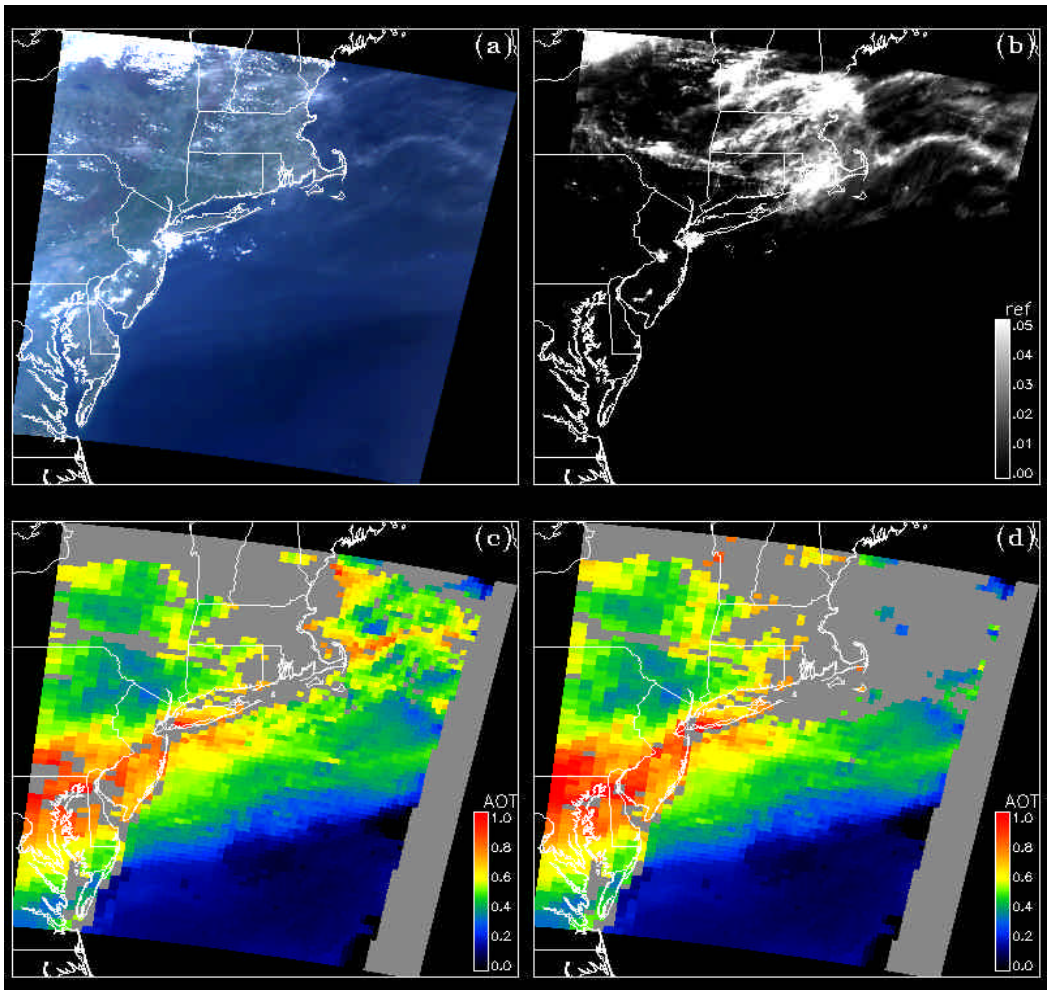

Figure. 6. (a): a color image (red: 0.66-μm channel; green: 0.55-μm channel; blue: 0.47 μm channel) processed from the MODIS data acquired over the northeastern part of the United States and the Atlantic Ocean at UTC 15:35 on May 5, 2001; (b): the 1.38-μm channel image over the same areas; (c): the aerosol optical depth (0.55 μm) image

retrieved with an earlier version of MODIS aerosol algorithm; and (d): the same as (c) but obtained with the current version of the aerosol algorithm, which includes the cirrus screening module and other improvements for aerosol retrievals over land.

Figure 6 shows an example of comparisons between aerosol optical depths retrieved with two versions of the aerosol algorithms – with and without the new cirrus screening module. Fig. 6a shows a color image (red: 0.66-μm channel; green: 0.55-μm channel; blue: 0.47 μm channel) of a MODIS scene. The data were collected over the northeastern part of the United States and the Atlantic Ocean at UTC 15:35 on May 5, 2001. Fig. 6b shows the 1.38-μm image for the scene. There are thin cirrus clouds in the upper portions of the image. Fig. 6c shows the image of aerosol optical depths at 0.55 μm derived with the earlier version of the operational aerosol algorithm. The thin cirrus clouds in the upper right portions of the image are incorrectly treated as aerosols during the retrievals. Fig. 6d shows the optical depth image obtained with the recent version of the aerosol algorithm, which includes the cirrus screening module and other improvements for aerosol retrievals over land surfaces. The upper right portions are successfully masked out and no aerosol retrievals were made over these areas

3 **Publications**:

Gao, B.-C., P. Yang, W. Han, R.-R. Li, and W. J. Wiscombe, An algorithm using visible and 1.38-micron channels to retrieve cirrus cloud reflectances from aircraft and satellite data, IEEE Transa. Geosci. Remote Sensing (in press).

Gao, B.-C., Y. J. Kaufman, D. Tanre, and R.-R. Li, Distinguishing tropospheric aerosols from thin cirrus clouds for improved aerosol retrievals using the ratio of 1.38-μm and 1.24-μm channels, Geophys. Res. Lett. (in press).

Yang, P., B.-C. Gao, W. J. Wiscombe, M. I. Mishchenko, S. Platnick, H.-L. Huang, B. A. Baum, Y. X. Hu, D. Winker, S.-C. Tsay, and S. K. Park, Inherent and apparent scattering properties of coated or uncoated spheres embedded in an absorbing host medium, Appl. Opt., 41, 2740 – 2759, 2002.

King, M. D., W. P. Menzel, Y. J. Kaufman, D. Tanre, B.-C. Gao, S. Platnick, S. A. Ackerman, L. A. Remer, R. Pincus, and P. A. Hubanks, Cloud, aerosol and water vapor properties from MODIS: preliminary results from Terra, submitted to IEEE Transa. Geosci. Remote Sensing in May 2002.

Gao, B.-C., P. Yang, R.-R. Li, S. K. Park, and W. J. Wiscombe, Detection of high clouds in polar regions during the daytime using the MODIS 1.375-μm channel, submitted to IEEE Transa. Geosci. Remote Sensing in May 2002.

Li, R.-R., Y. J. Kaufman, B.-C. Gao, and C. O. Davis, Remote sensing of suspended sediments and shallow coastal waters, Submitted to IEEE Trans. Geosci. Remote Sensing in June 2002.

Yang, P., H.-L. Wei, B. A. Baum, H.-L. Huang, A. J. Heymsfield, Y. X. Hu, B.-C. Gao, and D. D. Turner, The spectral signature of mixed-phase clouds composed of non-spherical ice crystals and spherical liquid droplets in the terrestrial window region, submitted to JQSRT in June 2002.

Staenz, K., J. Secker, B.-C. Gao, and C. O. Davis, Radiative transfer codes applied to hyperspectral data for the retrieval of surface reflectance, accepted for publication by the ISPRS Journal in 2002.